[9]J. L. Shay, E. Buehler, and J. H. Wernick, Phys. Rev. B 3, 2004 (1971).
[10]J. L. Shay and E. Buehler, Phys. Rev. B 3, 2598 (1971).
[11]C. C. Y. Kwan and J. C. Woolley, Can. J. Phys. 48, 2085 (1970); Phys. Status Solidi 44, K93 (1971); Appl. Phys. Letters 18, 520 (1971).
[12]J. Kavaliauskas, G. F. Karavaev, E. I. Leonov, V. M. Orlov, V. A. Chaldyshev, and A. Sileika, Phys. Status Solidi 45, 443 (1971).
[13]S. C. Abrahams and J. L. Bernstein, J. Chem. Phys. 55, 796 (1971).
[14]Von R. Sandrock and J. Treusch, Z. Naturforsch. 19a, 844 (1964).
[15]V. A. Chaldyshev and V. N. Pokrovskii, Izv. Vysshikh Uchebn. Zavedenii Fiz. 2, 173 (1960).
[16]J. J. Hopfield, J. Phys. Chem. Solids 15, 97 (1960).
[17]J. E. Rowe and J. L. Shay, Phys. Rev. B 3, 451 (1971).
[18]D. D. Sell, Appl. Opt. 9, 1926 (1970).
[19]E. Buehler, J. H. Wernick, and J. L. Shay, Mater. Res. Bull. 6, 303 (1971).
[20]S. Koeppen, P. Handler, and S. Jasperson, Phys. Rev. Letters 27, 265 (1971).
[21]A. S. Poplavnoi, Yu. I. Polpavnoi, and V. A. Chaldyshev, Izv. Vysshikn Uchebn. Zavedenii Fiz. 7, 17 (1970); 6, 95 (1970).

PHYSICAL REVIEW B VOLUME 6, NUMBER 4 15 AUGUST 1972

Electroreflectance and Band Structure of $Ga_xIn_{1-x}P$ Alloys

C. Alibert and G. Bordure
Centre d'Etude d'Electronique du Solide, 34 Montpellier, France

and

A. Laugier and J. Chevallier
Laboratoire de Physique des Solides, Centre National de la Recherche Scientifique, 92 Meudon, Bellevue, France

(Received 24 March 1972)

The electroreflectance spectra of solution-grown $Ga_xIn_{1-x}P$ alloys were measured at room temperature in the whole range of composition. The variation of the E_0, E_1, E_0', and E_2 energies with concentration is reported: It is parabolic for E_0 and E_1, and approximately linear for E_0' and E_2. Except for E_1 these results agree with the calculation of the band structure by the dielectric two-band method in the virtual-crystal approximation including the effect of disorder. The latter effect is found small. For E_1 the deviation from a linear variation is larger than calculated. E_1 exhibits another interesting anomaly: Its spin-orbit splitting is maximum for $x = 0.5$. The $\vec{k} \cdot \vec{p}$ method is used to calculate some band parameters from our data. The $\Gamma - X$ conduction-band crossover energy E_c and composition x_c are accurately determined using the E_0 vs x curve and the indirect gaps obtained from optical absorption: $x_c = 0.63 \pm 0.015$, $E_c = 2.14 \pm 0.01$ eV.

I. INTRODUCTION

The $Ga_xIn_{1-x}P$ semiconducting alloys form a continuous, single-phase, solid solution throughout the whole composition range. They have received increased attention recently because of the large direct band gap attainable. In these ternary alloys, direct transitions are possible with photon energies up to 2.15 eV, which makes it a potentially efficient electroluminescent source of light in the range of highest sensitivity of the human eye.[1-3]

The energy-band structures of GaP and InP have been calculated theoretically[4,5] and a large number of experimental results have yielded band-structure parameters. However, the band structure of $Ga_xIn_{1-x}P$ is not so well known. There has been disagreement about the value of the "crossover" composition x_c at which the energy of the Γ and X conduction-band minima becomes equal. From measurements on diodes, Lorenz *et al.*[2] determined $x_c = 0.8$. Measurements of the band-edge absorption coefficient as a function of photon energy by Rodot *et al.*[3] determined $x_c = 0.63$. This value has been confirmed by Williams *et al.*[6] and White *et al.*[7] using photoluminescence-excitation spectra, by Hakki *et al.*[8] using hydrostatic-pressure experiments and by photoluminescence at low temperature.[9] However, assigning the cathodo luminescence peaks at 300 °K to the band gap, some authors[10,11] give $x_c = 0.74$ with a parabolic-empirical variation of the direct band gap, $E_d = 1.34 + 1.426x + 0.758x(x-1)$. Onton and Chicotka[12] estimate that their low-temperature-photo-

luminescence spectra are consistent with these results. This bowing is considerably larger than previously reported.[3,7,9] In GaP and InP, the indirect gap $E_i = X_1^c - \Gamma_8^v$ is nearly the same, so that the disagreement on x_c is principally due to the discrepancy on the variation of the lowest direct-band-gap energy $E_d = \Gamma_6^c - \Gamma_8^v$ vs composition. An explanation was recently given[13] for this discrepancy, based on a reinterpretation of luminescence spectra.

Thus, there appears to be a need for directly measuring E_d and E_i with accuracy. In order to precisely determine the electronic structure of this system and to clarify the discrepancies outlined above, we have applied the modulation-spectroscopy technique to InP, GaP, and $Ga_xIn_{1-x}P$ alloys since it is generally recognized that this method represents the most accurate process presently available for determining transitions energies of interband critical points.[14]

The sharp optical structure obtained by modulation methods is usually not washed out by alloying in binary or pseudobinary solid solution. Electroreflectance (ER) data have been reported for some alloys,[15,16] particularly for the GaAs-InAs[17,18] and GaAs-GaP[19] systems. Thermoreflectance spectra were obtained on $Ga_xIn_{1-x}P$ by Lettington *et al.*,[20] but on thin epitaxial layers only. They were insufficiently resolved, however, probably because of the poor homogeneity and small thickness of the layers.

In this paper, an accurate determination of transition energies of interband critical points is made by performing ER experiments on high-purity and very homogeneous material at room temperature. Described in Sec. II are the sample growth, analysis, surface preparation, and the ER apparatus using an electrolyte electrode, derived from the technique of Shaklee, Pollak, and Cardona.[21] It was hoped that the high resolution inherent to the ER method would provide an accurate determination of the concentration dependence of the various gaps. For obtaining interband energies E_0 and E_1 with high accuracy, we have used in Sec. III the "three-point fit" of Aspnes and Rowe.[22] This method does not require optical constants or a Kramers-Kronig analysis and hence it is particularly suitable for new materials. The interpretation of the structure observed in the experimental spectra is aided in Sec. IV by recent improvements in energy-band calculation of alloys[23] and the knowledge of band structure and optical properties of GaP and InP.[4,5,24] The $\vec{k}\cdot\vec{p}$ method is used to calculate some band parameters from our data.

The band structure of $Ga_{0.63}In_{0.37}P$ so obtained is given by Fig. 1, which shows the location of the transitions responsible for the ER peaks of the typical spectrum illustrated by Fig. 2. E_0 is the fundamental-direct-optical threshold. The next higher threshold corresponds to the E_1 structure. Its exact location in k space is uncertain.[25,26] It is generally agreed that these transitions are in the [111] direction of the Brillouin zone and that the $\Lambda_6^c - (\Lambda_4^v, \Lambda_5^v)$ transitions are mainly responsible for the E_1 peaks although the $L_6^c - (L_4^v, L_5^v)$ transitions are almost degenerate with them. The metamorphism of critical points in this direction of the Brillouin zone, recently discussed,[27,28] obscures the exact origin of this transition.

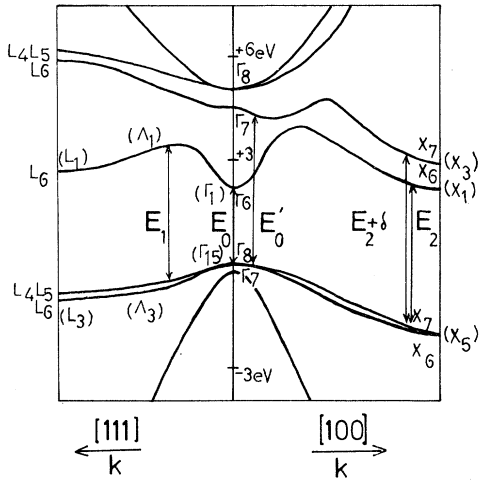

FIG. 1. Band structure of $Ga_xIn_{1-x}P$ with inclusion of the spin-orbit interaction for $x = x_c = 0.63$. The irreducible representations corresponding to the various orbital states are given in brackets. The double-group representations are given without brackets. In the text v and c are used to differentiate between valence and conduction band when there is more than one state of the same symmetry. The zero of energy is taken at the top of valence band.

The important results obtained here are the following ones (at room temperature):

(a) The E_0 gap ($\Gamma_6^c - \Gamma_8^v$) was measured through the whole composition range. A quadratic variation is obtained:

$$E_0 = 1.345 + 1.435x + 0.50x(x-1) .$$

The spin-orbit splitting Δ_0 was also measured through the entire concentration range. The value of Δ_0 for InP (0.10 eV) is nearly the same as for GaP. A linear law fits the variation of Δ_0 with x very well.

(b) The E_1 transition was followed continuously as a function of x. The variation is well represented by the quadratic form:

$$E_1 = 3.175 + 0.581x + 0.860x(x-1) .$$

The structure $E_1 + \Delta_1$ (Δ_1 is the spin-orbit splitting in the valence band) follows a similar law. For

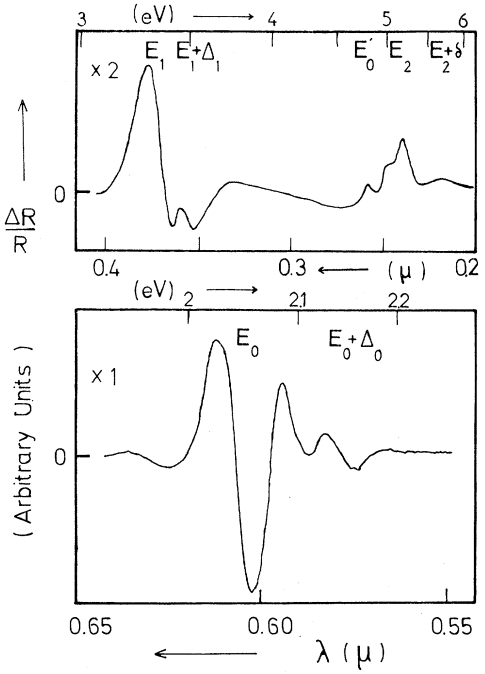

FIG. 2. Electroreflectance spectrum at room temperature of an alloy $Ga_xIn_{1-x}P$, $x = 0.57$.

$x = 0$, $E_1 + \Delta_1$ is well resolved ($E_1 + \Delta_1 = 3.19$ eV). The resolution decreases when x increases.

(c) The E_0' peak of InP (4.70 eV) varies smoothly as a function of x, tending to the 4.8-eV peak of GaP. The peaks E_2 $(X_1^c - X_5^v)$ and $E_2 + \delta$ $(X_3^c - X_5^v)$ were resolved; their variation in all the composition range is small, as is that of E_0'.

As expected, no structure assignable to the $X_1^c - \Gamma_8^v$ transitions appears in the ER spectra. For this reason, new optical-absorption measurements were performed. These are described in Sec. V. A new, more accurate determination of the crossover parameters is obtained:

$$x_c = 0.63 \pm 0.015 \quad \text{and} \quad E_c = 2.14 \pm 0.010 \text{ eV}.$$

II. EXPERIMENT

A. Sample Preparation

The growth of $Ga_xIn_{1-x}P$ is difficult for two reasons. The first is the high vapor pressure of phosphorus, the second is the high segregation coefficient of Ga. These two difficulties are avoided using a solution-growth method recently described.[29] An indium bath is continuously fed by phosphorus coming from vapor and by gallium from solid gallium phosphide. Very homogeneous crystals were obtained by this method in the whole range of compositions: Typically, on a length of 10 mm the variation of composition Δx can be lower than 0.08, as determined by electron microprobe. All crystals were undoped. The carrier concentration, given by Hall-effect measurements, was in the range 1×10^{16}–5×10^{16} cm^{-3}. Alloys were n type for $0 < x < 0.6$ and p type for $0.6 > x > 1$, lightly compensated. They were polycrystalline. Samples of about 800-μ thickness, obtained from ingots, were lapped on both sides and mechanically polished on one side with diamond paste down to 0.5-μ grain size. Then each specimen was analyzed by electron microprobe. For each point, the indium and gallium concentrations were simultaneously and independently measured. The total relative change in composition over the thickness of the sample and the surface of the specimen is estimated to less than 2%. Shortly before using, the specimens were lightly etched in a mixture of concentrated HCl and HNO_3 (1 : 4), and washed in distilled water before being transferred to the electrolytic cell. InP and GaP used as references in this work were grown in conditions similar to those of the alloys, as described in Ref. 30.

B. Electroreflectance Measurements

In the ER experiments the optical properties of samples are modulated by an electric field, generally created by a surface barrier.[14] This perturbation is synchronously detected by a lock-in amplifier. The quantity directly measured is the relative variation of reflectance $\Delta R/R$. A diagram of the experimental apparatus is shown in Fig. 3.

Light from a high-pressure xenon arc (Model No. XBO 450W) or a tungsten-filament lamp was focused on the entrance slit of a Jobin Yvon HRS-2 grating monochromator. The monochromatic light was focused on the sample, reflected at near normal incidence, and refocused on a photomultiplier (Model No. XP 1003 for the visible and near ultraviolet and Model No. 150 CVP for the infrared). The slit width gives a spectral resolution less than 10 Å.

A servomechanism acting on the power-supply voltage of the photomultiplier gives a nearly constant current detected by an electrometer (Keithley 602). The ac current is detected by a PAR Model No. HR8 lock-in amplifier. The ratio $\Delta R/R$ given by a multiplier (PAR Model No. 230) is connected to the Y axis of an XY chart recorder, while the X axis is supplied by a voltage, proportional to the wavelength λ, given by a precision potentiometer mechanically driven by the monochromator.

The modulating electric field was applied for our measurements at the interface between the semiconductor and an electrolyte. The electrolyte was a solution of KCl in water (1 : 10 M). The electrolyte cell was biased by a dc voltage and an ac square-wave voltage (200 Hz). The bias was adjusted to alloy composition and was typically about 1 V dc and ac.

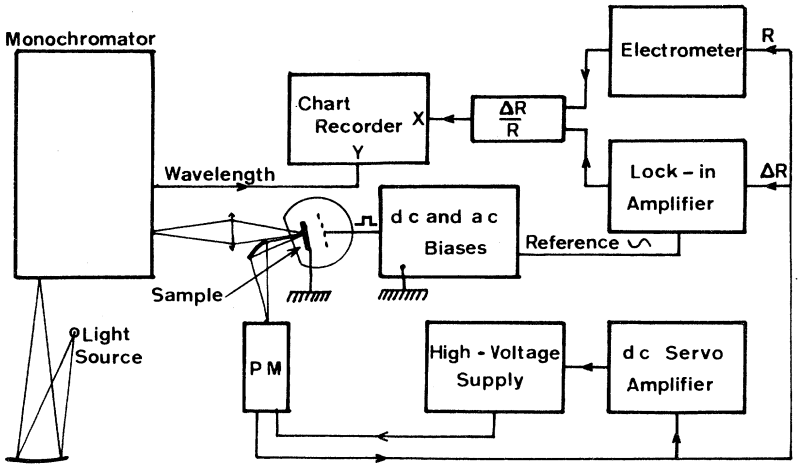

FIG. 3. Electroreflectance apparatus.

III. ANALYSIS OF EXPERIMENTAL SPECTRA

A. High-Resolution Interband-Energy Determination

A recent perturbation treatment of ER[31] has shown that the experimental line shape can be approximated quite well by

$$\Delta R/R = R_e\, C(E_d - \hbar\omega - i\Gamma)^n\, e^{i\theta}\,, \qquad (1)$$

where E_d is the energy of the direct threshold and C, θ, and Γ are the amplitude, phase, and broadening parameters, respectively. For the fundamental absorption edges modified by the Coulomb interaction, and for the three-dimensional critical points with large mass ratio, the best value for n is three, corresponding to a two-dimensional critical point. Using this value and the curve given by Aspnes and Rowes,[22] the energy transition is determined by the three-point fit, which is nearly independent of the physical model chosen to represent the transition and of the general experimental conditions.[32] The good agreement of the direct band gaps E_0 and E_1 of InP and GaP that we obtained, with previous measurements, confirms the accuracy of the method.

B. Results

1. General Features of Spectra

Pure InP and GaP and 11 samples of $Ga_xIn_{1-x}P$ alloys were measured in all the range of compositions. Figure 2 shows a typical ER spectrum of a $Ga_xIn_{1-x}P$ alloy ($x = 0.57$).

At low energy (1.3–3 eV) there appears a very sharp structure corresponding to the direct fundamental threshold E_0. Some indication of impurity effects giving a peak below E_0 appears on some spectra for low x, as previously observed in InP[24] and GaAs.[18,24] This peak has a very different ac and dc voltage dependance. It can be eliminated by convenient bias and is not discussed here. With the doping used here, no Burstein-Moss shift is to be considered. A less sharp structure (E_1 transition) is seen in the range 3–4 eV. The broadening increases regularly from $x = 0$ to $x = 1$ as previously observed for $GaAs_{1-x}P_x$.[19] These E_0 and E_1 structures are sufficiently sharp to allow an accurate determination of the energies and their composition variations. At higher energies (4.5–6 eV) smaller peaks appear. They are less well resolved than the low-energy peaks; their energy has a relatively small variation with x.

2. Low-Energy Transitions: InP *and* GaP

On Fig. 4 we can see the lower part of the ER spectrum of an n-type InP sample ($N_D - N_A = 5\times10^{16}$ cm^{-3}) at room temperature. The structure between 1.30 and 1.40 eV (0.90 and 0.95 μ) corresponds to the fundamental absorption edge. The three-point method gives the value 1.345 ± 0.002 eV. This value agrees well with previous measurements.[24,33] The structure between 1.40 and 1.50 eV (0.82 and 0.87 μ) corresponds to the spin-orbit interaction in the valence band. This peak is well separated from the previous one and an accurate determination of Δ_0 is possible, giving $\Delta_0 = 100 \pm 5$ meV.[34]

A higher-energy structure appears between 3 and 3.5 eV (0.40 and 0.35 μ, Fig. 5). It corresponds to the E_1 and $E_1 + \Delta_1$ transitions. The three-point fit gives $E_1 = 3.175 \pm 0.008$ eV and $\Delta_1 = 125 \pm 15$ meV. These determinations are less accurate than for E_0 and $E_0 + \Delta_0$ because of the overlap of E_1 and Δ_1 structure.

In Fig. 4 we can see the low-energy part of an ER spectrum of undoped GaP. The smallest direct absorption edge E_0 and its split-off component $E_0 + \Delta_0$ are responsible for the structure between 0.4 and 1.5 μ (2.6 and 3 eV). The values obtained are $E_0 = 2.780 \pm 0.006$ eV and $\Delta_0 = 105 \pm 15$

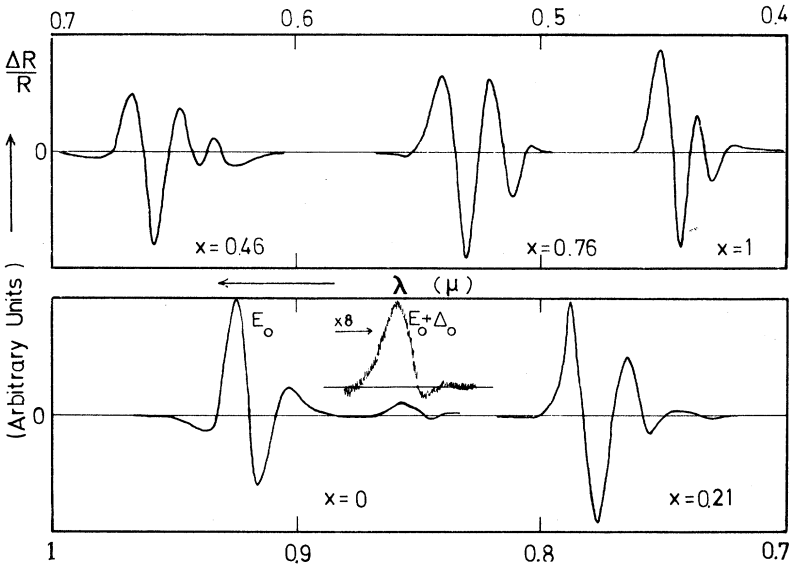

FIG. 4. ER spectra showing E_0 and $E_0+\Delta_0$ transitions for $Ga_xIn_{1-x}P$ at room temperature.

meV. The spin-orbit splitting obtained is in good agreement with the results of Subashiev and Abagyan,[35] of Thompson *et al.*,[19] of Cardona *et al.*,[24] and of recent measurement at 25 °K.[36] The value of E_0 is quite accurate compared to the transmission, 2.78 eV[37] and 2.76 eV,[35] photoconductivity, 2.79 eV,[38] and reflectivity, 2.80 eV,[39] measurements. As expected, no effect due to the indirect edge at 2.25 eV is seen. A structure at higher energy is assignable to E_1 and $E_1+\Delta_1$. The values are $E_1 = 3.760 \pm 0.010$ and $E_1+\Delta_1 = 3.86 \pm 0.03$ eV. These peaks correspond to the structure observed in the reflexion spectrum at 3.7 eV.[24,39-41] The splitting Δ_1 is not well resolved, due probably to the fact that it becomes comparable with the linewidth. These results about E_0, E_1, Δ_0, and Δ_1 agree with previous ER measurements.[19,24]

3. *Low-Energy Transitions:* $Ga_xIn_{1-x}P$

The spectra of alloys are quite similar to those of InP and GaP. Figures 4 and 5 show the ER spectra for the low-energy E_0 and E_1 transitions, respectively. The E_0, the split-off $E_0+\Delta_0$, and the E_1 peaks are clearly resolved for all x values. The spin-orbit splitting Δ_1 is less resolved when x goes up to 1.

Figure 6 shows the variation of the direct energy gap and its split-off component $E_0+\Delta_0$ as a function of x. Using the method described later for E_1, the best fit is obtained by a parabolic variation $E_0 = 1.345 + 1.435x + 0.50x(x-1)$. A similar law describes the variation of $E_0+\Delta_0$ as shown on Fig. 6, where the solid line corresponds to a constant value of Δ_0: 0.1 eV. However, a best fit is obtained with a linear variation of Δ_0 with x: $\Delta_0 = 0.11 - 0.02x$ (dashed curve).

The E_1 and $E_1+\Delta_1$ structures of InP are continuously observed in the whole range of compositions up to GaP. The variation is not linear. Assuming a quadratic variation[23]

$$E = a + bx + cx(x-1), \tag{2}$$

we determine the bowing parameter c.

In Fig. 7 the deviation from linearity of the transition energies E_1, determined by the three-point method, is plotted as a function of $x(1-x)$. The expected quadratic deviation appears as a straight line, determining $c = 0.86 \pm 0.06$ eV. It is seen that the determination of c is relatively accurate. The resulting equation for $E_1(x)$ is $E_1 = 3.18 + 0.58x + 0.86x(x-1)$ and is plotted on Fig. 8 together with experimental points.

For $x > 0.2$ due to the overlap of structure, it is difficult to apply the three-point-fit method to the determination of Δ_1, particularly for $x > 0.7$ where the $E_1+\Delta_1$ structure is weak. The difficulty is the same for the GaS-GaP system.[19] But, generally, one peak only is then assignable to $E_1+\Delta_1$ and we use the energy of this peak to determine Δ_1. The variation of Δ_1 with x is continuous but not linear, as seen on Fig. 8. We observe a maximum for $x = 0.5$; the departure from linearity is large: 0.07 eV; and the parabolic law, $\Delta_1 = 0.13 - 0.03x + 0.28x \times (1-x)$, can fit the data. This is surprising since a linear variation is expected, as for Δ_0. However, a similar variation was also observed in some other systems[16,18,19] with a smaller departure from linearity. Table I summarizes the obtained results.

4. *High-Energy Structures*

For InP, peaks at 4.7, 5, and 5.6 eV appear. For GaP the corresponding peaks are at 4.8, 5.3,

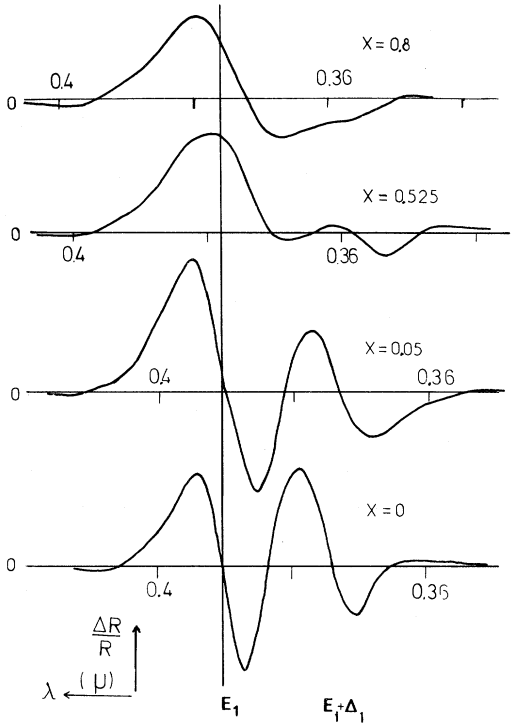

FIG. 5. ER spectra showing E_1 and $E_1+\Delta_1$ transitions for $Ga_xIn_{1-x}P$ at room temperature. Spectra are shifted in order to take as a reference (E_1 line) the wavelength corresponding to the E_1 transition, as determined by the three-point-fit method. With this representation the line broadenings can be directly compared. Particularly, no important broadening appears from $x=0$ to $x=0.05$. The increasing of spin-orbit splitting Δ_1 with x, up to 0.5 is also visible.

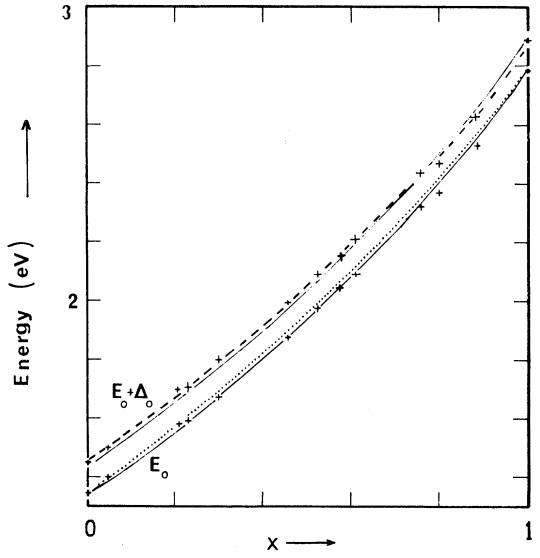

FIG. 6. Variation of direct thresholds E_0 and $E_0+\Delta_0$ with x in $Ga_xIn_{1-x}P$ at room temperature. A parabolic law $E_0=a+bx+cx(x-1)$ fits the data. The solid line corresponds to the experimental value $c=0.50$ eV. The dotted line corresponds to the intrinsic bowing $c_i=0.37$ eV calculated in the virtual-crystal approximation. A similar law describes the variation of $E_0+\Delta_0$. The solid line corresponds to a constant value of the spin-orbit splitting 0.1 eV. A best fit is obtained with a linear variation, $\Delta_0=0.11-0.02x$, by the dashed curve.

and 5.7 eV. (The estimated error is ±0.04 eV.) They correspond to previously reported peaks attributed to the E_0', E_2, and $E_2+\delta$ transitions, respectively.[24,42] Within experimental uncertainties the concentration dependence is linear. For instance the spectrum of Fig. 2 gives for $x=0.57$: $E_0'=4.78$, $E_0'+\Delta_0'$ (?) $=5.04$, $E_2=5.20$, $E_2+\delta=5.65$ eV. By comparison with GaP, InP,[24] and $GaAs_{1-x}P_x$[19] it is reasonable to assume that the main contribution to E_0' comes from a region of k space in the [100] direction near $k=0$. However, the energy of E_0' represents the value of the $\Gamma_7^c-\Gamma_8^v$ gap since the corresponding conduction and valence bands are almost parallel in this direction near $k=0$. E_2 and $E_2+\delta$ are attributed to $X_1^c-X_5^v$[24,33] and $X_3^c-X_5^v$ transitions.[24]

IV. DISCUSSION

A. Line Broadening

As seen in Figs. 4 and 5 giving $\Delta R/R$ vs λ, there is no significant change of structural shape with composition of the fundamental edge as in the case of E_1. This fact seems to eliminate a systematic change in the surface-barrier structure with composition. The structural shape in the alloys is very similar to that of the constituent compounds and no important broadening appears, indicating that there is a good macroscopic homogeneity, that the microscopic disorder is not a significant source of lineshape distortion, and that there is no impurity ef-

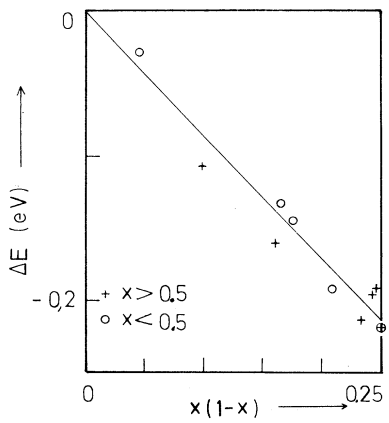

FIG. 7. Departure from linearity ΔE for the E_1 transitions.

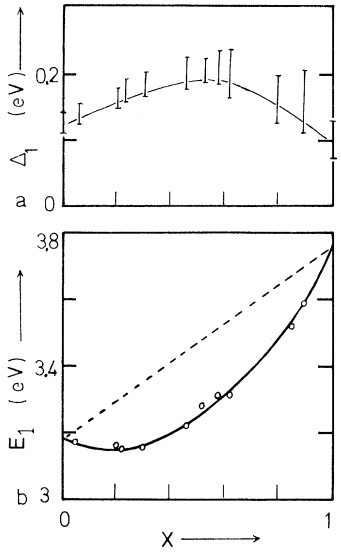

FIG. 8. Variation of E_1 (a) and of spin-orbit splitting Δ_1 (b) vs x.

fect. The broadening is approximately proportional to the energy, which is quite natural.

For the substitutional alloy considered here, the random arrangement of Ga and In on III-atom sites could cause a tailing in the density of states inside the forbidden region at the band edge, as found in second- and higher-order perturbation calculations.[43,44] This would apparently imply that the broadening changes quickly in alloys close to the pure compounds. We have especially studied the alloy with $x = 0.05$. No important change is visible for the E_0 spectrum and for the E_1 spectrum. Figure 5 shows a small increase of broadening of about 10% only. This is consistent with previous results on the GaAs-InAs[18] and GaSb-InSb[16] systems.

B. Application of the Dielectric Theory to $Ga_xIn_{1-x}P$ Alloys

As shown by the virtual-crystal model,[45] taking account of[43,44] the periodic part of the potential, and by the perturbation calculations accounting for the effects of random fluctuations in the potential, a one-electron band structure is a good description of the electronic structure of alloys, as for the constituents. Van Vechten and Bergstresser have found that the dielectric method gives good agreement with experiment, but that the local-pseudopotential method apparently does not yield satisfactory results for the calculation of the band structure of alloys. They predicted a nonlinear dependence of the interband gaps on concentration. In $Ga_xIn_{1-x}P$ alloys our ER measurements show, in agreement with the thermoreflectance data,[20] an approximately quadratic dependence, as in many semiconducting systems[16,17] and as predicted by the theory.[23]

We have applied this dielectric method to $Ga_xIn_{1-x}P$. The Vegard's law is obeyed in this system, within experimental uncertainties.[10,46] We have adjusted the parameters of the theory, in particular the average valence-band to d-band f sum D_{av}[5,47] characterizing nonlocal effects, so as to agree with experiment for E_0 and E_1 in InP and GaP. These values are given in Table II. The corresponding calculated values of the bowing parameter c [Eq. (2)] are compared with experiment in Table III. The intrinsic bowing c_i is found in the virtual-crystal approximation. The extrinsic bowing $c_e = 0.31$, due to the effect of aperiodicity, was calculated in Ref. 23 for the E_0 lowest direct gap and for the higher-vertical-point direct gaps E_1 and E_2, connecting the same two bands. For E_0' and $E_2' + \delta$, c_e was estimated zero by comparison with $GaAs_{1-x}P_x$.[19-23] The total calculated bowing is assumed to be $c_i + c_e$.

It is interesting to remark that all calculated bowing parameters are larger than experimental values except for E_1. This fact is to be compared with the anomalous variation of Δ_1 with x and will be discussed later. It seems that the disorder effect is smaller than predicted, as previously men-

TABLE I. $\Gamma_1^c - \Gamma_{15}^v$ and $\Lambda_1^c - \Lambda_3^v$ data for $Ga_xIn_{1-x}P$ alloys (energies in eV).

	E_0	$E_0+\Delta_0$	$E1$	$E_1+\Delta_1$
0	1.345 ± 0.002	1.446 ± 0.004	3.175 ± 0.008	3.30 ± 0.008
0.05	1.400 ± 0.002	1.500 ± 0.005	3.175 ± 0.01	3.31 ± 0.01
0.21	1.585 ± 0.003	1.698 ± 0.007	3.159 ± 0.01	3.33 ± 0.02
0.23	1.589 ± 0.003	1.702 ± 0.010	3.154 ± 0.01	3.33 ± 0.02
0.30	1.671 ± 0.003	1.800 ± 0.010	3.154 ± 0.01	3.34 ± 0.03
0.46	1.872 ± 0.003	1.974 ± 0.007	3.220 ± 0.01	3.42 ± 0.02
0.525	1.976 ± 0.004	2.092 ± 0.008	3.279 ± 0.015	3.47 ± 0.02
0.57	2.042 ± 0.004	2.145 ± 0.008	3.306 ± 0.015	3.52 ± 0.02
0.615	2.090 ± 0.003	2.205 ± 0.007	3.314 ± 0.010	3.52 ± 0.03
0.76	2.326 ± 0.004	2.436 ± 0.009		
0.80	2.365 ± 0.005	2.466 ± 0.010	3.482 ± 0.015	3.64 ± 0.04
0.885	2.525 ± 0.005	2.628 ± 0.010	3.589 ± 0.010	3.76 ± 0.04
1	2.777 ± 0.006	2.885 ± 0.010	3.756 ± 0.010	3.86 ± 0.02

TABLE II. Values of the lattice parameter d, the nonlocal parameter D_{av} and the antisymmetric potential C used for the dielectric-method calculation. Comparison of calculated and experimental values for InP and GaP.

Crystal	d(Å)	C(eV)	D_{av}	E_0(eV) calc	E_0(eV) expt	E_1(eV) calc	E_1(eV) expt
GaP	4.460	3.30	1.155	2.72	2.78	3.82	3.76
InP	4.802	3.34	1.273	1.36	1.345	3.165	3.175

tioned in the discussion on broadening. This is especially surprising since the large mismatch of lattice constants should facilitate clustering and microinhomogeneities. The good quality and homogeneity of the sample are confirmed.

C. Spin-Orbit Splittings Δ_0 and Δ_1

We follow the well-known "time sharing" principle which was applied by Kane[48] for estimating spin-orbit splittings in crystals from a knowledge of these splittings in the constituent free atoms. The spin-orbit splitting Δ_0 of the valence band at Γ_{15} is given by

$$\Delta_0=\left(\frac{3\hbar i}{4mC^2}\right)\left\langle\Gamma_{15}^{(x)}\left|\frac{\partial V}{\partial x}P_y-\frac{\partial V}{\partial y}P_x\right|\Gamma_{15}^{(y)}\right\rangle . \qquad (3)$$

V is the self-consistant crystal potential, p the linear-momentum operator. $|\Gamma(i)\rangle$ are the wave functions, which define the Γ_{15} representation (without splitting). It is expected that most of the contribution to the matrix element in Eq. (3) is given by the wave functions near the cores and hence that Δ_0 is given by a contribution from the group-III atoms and by another one from the group-V atoms. The core potential and wave function near the core are thought not to be drastically affected by the neighboring atoms. Generalizing for ternary III-V alloys, the Braunstein-Kane approximation[49] is written

$$\Delta_0=[x\xi_{Ga}\Delta_{Ga}+(1-x)\xi_{In}\Delta_{In}+\xi_P\Delta_P]C . \qquad (4)$$

The normalization constant C was found to be 29/20 for III-V compounds.

Δ_i is the one-electron spin-orbit splitting of ion i. The coefficients ξ are related to the ionicity of the compounds and indicate the relative fraction of each constituent atom which enters in Δ_0. For all group-III atoms the value 0.35 was suggested.[49] Equation (4) predicts a linear variation of Δ_0 with x as observed within experimental uncertainties.

The spin-orbit splitting Δ_1 at Λ_3 is given by an equation similar to Eq. (3),[50,51] where the wave functions $|\Lambda_3(i)\rangle$ which define the representation are used. A factor $\frac{2}{3}$ is to be used, due to the fact that Γ is a triply-degenerate orbital state and Λ is a doubly degenerate orbital state.[25]

Using the same discussion as for Δ_0, and the fact that the matrix element is roughly the same as for Δ_0 and is also independent of the position of Λ along the [111] direction,[4,52] a linear variation with x is also expected for Δ_1. As seen in Sec. III the curve plotted through the points in Fig. 8(b) is only an estimated one because of the great uncertainties on Δ_1 values. However, the precision is sufficient to conclude that the $\frac{2}{3}$ spin-orbit-splitting rule is not obeyed for GaP-InP (as previously remarked for GaP and InP[19,24] and that the departure from linearity is large. It was suggested[19,53] that this variation is due to a sliding in k space of the Λ critical point. Thompson *et al.*[19] suggested that the large value of Δ_1 may be due to an increasing cationic proportion ξ_{III} of the valence-band wave functions as one moves away from $k=0$ in the L direction. Then Eq. (3) gives a higher value of the splitting. With $\xi_{III}=0.5$ and with $\Delta_P=0.046$, $\Delta_{In}=0.27$, $\Delta_{Ga}=0.12$ eV,[49] we obtain $\Delta_1=0.15$ and 0.08 eV for InP and GaP, respectively, which agrees with our data within estimated errors: Δ_1(InP) = 0.12, Δ_1(GaP) = 0.10 eV. It is obvious that a convenient sliding along the L direction can explain the departure from linearity of $\Delta_1(x)$. If we assume for ξ_{III}, in the range $x>0.5$, the value which gives the best fit for GaP, Eq. (4) gives $\Delta_1=155$ meV for $x=0.5$. It can be objected that the present estimation is very rough, but refined calculations, such as the relativistic orthogonalized

TABLE III. Comparison between experimental and calculated values of bowing parameters c(eV) at 300 °K for direct transitions, at 300 °K, in $Ga_xIn_{1-x}P$. c_i is the intrinsic bowing, given in the "virtual-crystal" approximation; c_e is the extrinsic bowing taking account of the disorder effect in the Van Vechten–Bergstresser model.

	c_i	c_e	c(calc)	c(expt)
E_0	0.37	0.31	0.68	0.50 ± 0.05
E_1	0.27	0.31	0.58	0.86 ± 0.06
E_2	0.10	0.31	0.41	± 0.15
$E_2+\delta$	0.13	0.00	0.13	± 0.15
E_0'	0.16	0.00	0.16	± 0.15

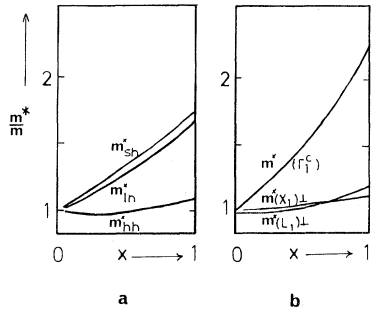

FIG. 9. Calculated variation of effective masses (in units of free-electron mass m) for holes (a) and electrons (b).

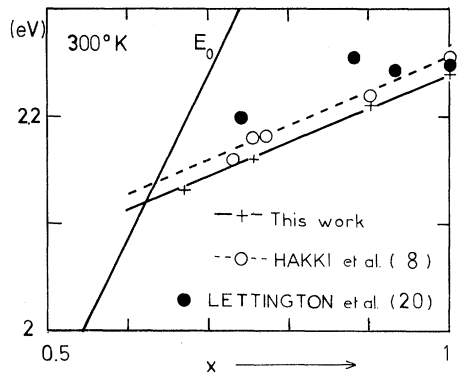

FIG. 10. Determination of the crossover values (at 300 °K) using E_0 and the values of indirect band gap E_i given by optical absorption. The values of electrotransmission (Ref. 20) are also given for comparison.

plane-wave model, do not give best fits.[54] The large departure from linearity of $\Delta_1(x)$ seems to be due to the small anionic contribution because of the particularly small value of Δ_P. It can be assumed then that this departure is larger for GaP-InP than for GaAs-InAs and for the latter than for GaSb-InSb. The comparison of our data with the data for these two systems[18,16] confirms this assumption.

D. Band Parameters

The effective mass at the Γ_{15} conduction-band point can be calculated, using the $\vec{k}\cdot\vec{p}$ method[48] as described by Cardona,[55] taking account of the interacting states Γ_{15c}, Γ_{15v}, and the spin-orbit splitting of the Γ_{15v}. We use our experimental data for E_0, Δ_0, and E_0'. The same method can be used to estimate the transverse effective masses at L_{1c} and L_{3v}, using our data for E_1, Δ_1, and the constant value 7 eV for E_1'.[4] The transverse effective mass at X_1 can also be estimated from the E_2 gap determined experimentally: from $m_\perp^{-1}(X_{1c}) = 1 + 19/E_2$.[55]

The results of these calculations are plotted on Fig. 9(b). The effective masses of holes are also determined [Fig. 9(a)], using the parameters A, B, C^2 of Dresselhauss *et al.*[55,56]: m_{hh}^*, m_{lh}^*, and the split-off band mass m_{sh}^*. In Fig. 9 InP is taken as reference. We have, in units of free-electron mass: $m^*(\Gamma_{1c}) = 0.074$ (experimental values: 0.073,[57] 0.077 [58]), $m_\perp^*(L_{1c}) = 0.15$, $m_\perp^*(X_1) = 0.21$, $m_{hh}^* = 0.43$, $m_{sh}^* = 0.12$, $m_{lh}^* = 0.078$.[59]

V. INDIRECT BAND GAP

The accuracy of our measurements should allow the determination of the exact crossover parameters since their value depends more upon direct band gaps than indirect ones, as previously indicated. Indirect transitions were not seen in ER spectra. This was expected because of the smooth variation of E_i with $h\nu$ near E_g. Absorption measurements allow us to obtain these values. Using this technique H. Rodot *et al.*[3] have determined the band structure of these alloys. We have performed some measurements to state more precisely the indirect band-gap values E_i.

Samples were lapped so that the condition $\alpha d \simeq 1$ was always respected (d = thickness, α = absorption coefficient). The gap was given by extrapolation of straight lines obtained from the well-known expression $\alpha^{1/2} \propto (\hbar\omega - Eg)$ for allowed indirect transitions with the constant value $R = 0.27$ for reflectivity. The band gap of GaP was found to be 2.24 eV. Results are plotted on Fig. 10. We have reported also the value of Hakki *et al.*[8] By observing the displacement of absorption edge in the alloys from that of GaP and assuming a band-gap energy of 2.26 eV for the latter, these authors obtain somewhat higher values than ours; however, the variation dE_g/dx is the same. From thermotransmission measurements, inaccurate values of indirect band gap were given by Lettington *et al.*[20] Inaccuracy, certainly, came from inhomogeneity in composition along the depth. Comparing with our previous photoluminescence results,[9,10] we see that the variation of indirect gaps with composition at 300 °K is larger than that at 4 °K. At 300 °K the slope dE_i/dx is 3.2 meV/at.% whereas at 4 °K it is 0.4 meV/at.%. The intersection of the indirect-gap line with our $E_0(x)$ curve gives $x_c = 0.63 \pm 0.015$ and $E_c = 2.14 \pm 0.01$ eV at 300 °K, confirming the values given in Refs. 3 and 8. These values well agree with recent results obtained by Bachrach and Hakki[61] from absorption and photoluminescence measurements. We think, however, that our values are more accurate.

Using these determinations of E_i, the band parameters calculated in Sec. IV and our ER data and taking as reference the band structure calculated by the $\vec{k}\cdot\vec{p}$ method for GaP and InP,[4] we can know the detailed band structure of $Ga_xIn_{1-x}P$ alloys. The band structure of the particular alloy corresponding to the $\Gamma - X$ crossover is given by Fig. 1.

[1]C. Hilsum and P. Porteous, in *Proceedings of the International Conference on Physics of Semiconductors, Moscow* (Nauka, Leningrad, 1968), p. 1214.

[2]M. R. Lorenz, W. Reuter, W. P. Dumke, R. J. Chicotka, G. D. Petit, and J. M. Woodall, Appl. Phys. Letters, 13, 42 (1968).

[3]H. Rodot, J. Horak, G. Rouy, and J. Bourneix, Compt. Rend. 269B, 381 (1969).

[4]F. H. Pollak, G. W. Higgibotham, and M. Cardona, J. Phys. Soc. Japan, Suppl. 21, 20 (1966).
[5]J. A. Van Vechten, Phys. Rev. 187, 1007 (1969).
[6]E. W. Williams, A. M. White, A. Ashford, C. Hilsum, and P. Porteous, J. Phys. C 3, L55 (1970).
[7]A. M. White, E. W. Williams, P. Porteous, and C. Hilsum, J. Phys. D 3, 1322 (1970).
[8]B. W. Hakki, A. Jayaraman, and C. K. Kim, J. Appl. Phys. 41, 5291 (1970).
[9]J. Chevallier and A. Laugier, Phys. Status Solidi 8, 437 (1971).
[10]A. Onton, M. R. Lorentz, and W. Reuter, J. Appl. Phys. 9, 3420 (1971).
[11]M. R. Lorentz and A. Onton, in *Proceedings of the Tenth Conference on Physics of Semiconductors, Cambridge, Mass.*, edited by S. P. Keller, J. C. Hensel, and F. Stern (U. S. AEC, Oak Ridge, Tenn., 1970), p. 144.
[12]A. Onton and R. J. Chicotka, Phys. Rev. B 4, 1847 (1971).
[13]A. Laugier and J. Chevallier, Solid State Commun. 10, 353 (1972).
[14]M. Cardona, *Modulation Spectroscopy* (Academic, New York, 1969).
[15]J. S. Kline, F. H. Pollak, and M. Cardona, Helv. Phys. Acta 41, 968 (1968).
[16]S. S. Vishnubhatla, B. Eyglument, and J. C. Woolley, Can. J. Phys. 47, 1661 (1969).
[17]A. G. Thompson and J. C. Woolley, Can. J. Phys. 45, 2597 (1967).
[18]E. W. Williams and V. Rehn, Phys. Rev. 172, 798 (1968).
[19]A. G. Thompson, M. Cardona, K. L. Shaklee, and J. C. Wooley, Phys. Rev. 146, 601 (1966).
[20]A. H. Lettington, D. Jones, and R. S. Sarginson, J. Phys. C 4, 1534 (1971).
[21]K. L. Shalkee, F. H. Pollak, and M. Cardona, Phys. Rev. Letters 15, 883 (1965).
[22]D. E. Aspnes and J. E. Rowe, Phys. Rev. Letters 4, 188 (1971).
[23]J. A. Van Vechten and T. K. Bergstresser, Phys. Rev. B 1, 3351 (1970).
[24]M. Cardona, K. L. Shaklee, and F. H. Pollak, Phys. Rev. 154, 696 (1967).
[25]M. Cardona, in *Proceedings of the International Conference on Physics of Semiconductors, Paris*, edited by M. Hulin (Dunad, Paris, 1964), p. 181.
[26]E. O. Kane, Phys. Rev. 146, 558 (1966).
[27]D. E. Aspnes and J. E. Rowe, in Ref. 11 p. 422.
[28]S. Jasperson, S. Koeppen, and P. Handler, in Ref. 11, p. 432.
[29]A. Laugier and J. Chevallier, Phys. Status Solidi 7, 427 (1971).
[30]H. Rodot, A. Hruby, and M. Schneider, J. Cryst. Growth 3, 305 (1968).
[31]D. E. Aspnes and J. E. Rowe, Solid State Commun. 8, 1145 (1970).
[32]C. Alibert and G. Bordure (unpublished). By use of a heterojunction Cu_2Se-Ge as a surface-barrier device, the validity of this method was controlled and the value of the Ge gap was obtained with a precision better than 1 meV for any bias conditions, especially with very low biases.
[33]D. L. Greenaway, Phys. Rev. Letters 9, 97 (1962).
[34]This result agrees with a previous determination (Ref. 24) but is somewhat smaller than the observations in $CdSnP_2$; see J. E. Rowe and J. L. Shay, Phys. Rev. B 3, 451 (1971).
[35]W. K. Subashiev and S. A. Abagyan, in Ref. 25, p. 225.
[36]D. D. Sell and P. Lawaetz, Phys. Rev. Letters 26, 311 (1971).
[37]P. J. Dean, G. Kaminski, and R. B. Zetterstrom, J. Appl. Phys. 38, 3551 (1967).
[38]D. F. Nelson, L. F. Johnson, and M. Gerhenzen, Bull. Am. Phys. Soc. 9, 236 (1964).
[39]R. Zallen and W. Paul, Phys. Rev. 134, 1628 (1964).
[40]T. K. Bergstresser, M. L. Cohen, and E. W. Williams, Phys. Rev. Letters 15, 662 (1965).
[41]J. C. Woolley, A. G. Thomson, and M. Rubenstein, Phys. Rev. Letters 15, 670 (1965).
[42]Reference 14, p. 244.
[43]R. H. Parmenter, Phys. Rev. 97, 587 (1955).
[44]M. Cutler and N. F. Mott, Phys. Rev. 181, 1336 (1969).
[45]L. Nordheim, Ann. Physik 9, 607 (1931); 9, 641 (1931).
[46]L. M. Foster and J. E. Scardefield, J. Electrochem. Soc. 117, 934 (1970).
[47]J. A. Van Vechten, Phys. Rev. 182, 891 (1969).
[48]E. O. Kane, J. Phys. Chem. Solids 1, 82 (1956).
[49]R. Braustein and E. O. Kane, J. Phys. Chem. Solids 23, 1423 (1962).
[50]M. Cardona and D. L. Greenaway, Phys. Rev. 125, 1291 (1961).
[51]M. Cardona, in *Semiconductors and Semimetals* (Academic, New York, 1967), Vol. 3, p. 142.
[52]C. W. Higginbotham, F. H. Pollak, and M. Cardona, in Ref. 1, p. 57.
[53]Reference 14, p. 283.
[54]G. G. Wepfer, T. C. Collins, and R. N. Euwema, Phys. Rev. B 4, 1296 (1971).
[55]M. Cardona, J. Phys. Chem. Solids 24, 1943 (1963); 26, 1351 (1965).
[56]G. Dresselhauss, A. F. Kip, and C. Kittel, Phys. Rev. 98, 368 (1955).
[57]T. S. Moss and A. K. Walton, Physica 25, 1142 (1959).
[58]E. D. Palik and R. F. Wallis, Phys. Rev. 123, 131 (1961).
[59]The recent improvement over Cardona's method, [P. Lawaetz, Phys. Rev. B 4, 3460 (1971)] gives results slightly different but the variation of m^*'s vs x is not significantly changed.
[60]J. Chevallier and H. Rodot, Compt. Rend. 271B, 1037 (1970).
[61]R. Z. Bachrach and B. W. Hakki, J. Appl. Phys. 12, 5102 (1971).